

EXPERIMENTAL INVESTIGATION OF FLOW PAST FINITE BLUNT PLATES USING PROPER ORTHOGONAL DECOMPOSITION

Liu Liu Shi

Department of Mechanical Engineering,
Shanghai Jiao Tong University
800 Dongchuan Rd., Shanghai, 200240, China
vie@sjtu.edu.cn

Jun Yu

Department of Mechanical Engineering,
Shanghai Jiao Tong University
800 Dongchuan Rd., Shanghai, 200240, China
mmlal@163.com

Ying Zheng Liu (Corresponding author)

Department of Mechanical Engineering,
Shanghai Jiao Tong University
800 Dongchuan Rd., Shanghai, 200240, China
yzliu@sjtu.edu.cn

ABSTRACT

In this study, PIV measurements of flow past finite blunt plates with length-to-thickness ratio $L/D = 3, 6,$ and 9 were performed in a low speed water channel. The Reynolds number was $Re_D = 1000$ based on the plate's thickness, D . Detailed examination of the flow past finite blunt plates with different length-to-thickness ratios displayed different flow characteristics. The large scale structures were found to make great contribution to the unsteadiness of the flow. Proper orthogonal decomposition (POD) analysis using 500 realizations of PIV velocity fields were performed to identify the dominant flow structures.

INTRODUCTION

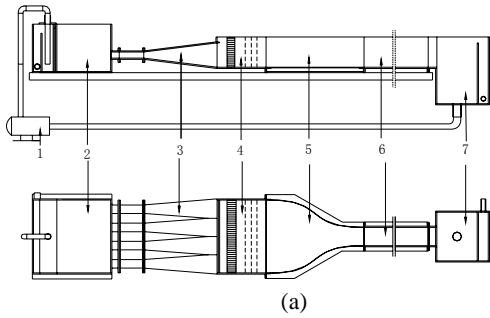
The finite blunt plate is a common configuration found in many structures, such as bridge decks, high-rise buildings, heat sinks in electronic equipments. Despite of its simple geometry, the flow past finite blunt plates has received increasing attention since it is associated with a lot of engineering problems like flow-induced vibration, flow-structure interactions, intensified heat and fluid transfer. The flow separates from the leading edge and not always reattaches on the plate's surface, depending on the plate length-to-thickness ratio L/D , L is the length of the plate and D is the plate's thickness. The flow patterns will be totally different for plates of different ratios. Numerous efforts have been made, both experimentally and numerically, to study the characteristics of the separated and reattaching flow over finite blunt plates (Parker and Welsh, 1983; Nakamura et al., 1991; Ohya et al., 1992; Hourigan et al., 2001; Mills et al., 2003). However, no detailed

description of the global features of this type of flow has been reported. In the present study, PIV measurements were carried out in a low-speed water channel at a Reynolds number $Re_D = 1000$ to study the flow characteristics in more detail. A high-resolution CCD Camera (RedLake, USA) with 11 Mega pixels was used in experiments, enabling a detailed view of the wake at the spatial resolution of the vectors $0.47 \text{ mm} \times 0.47 \text{ mm}$. Three cases, e.g., $L/D = 3, 6, 9$, were adopted so that each case corresponds to a different shedding mode (Nakamura et al., 1991; Ohya et al., 1992) showing different features. Furthermore, Proper Orthogonal Decomposition (POD) analysis was performed on 500 PIV realizations to shed more light on the flow structures which modulate the global features.

EXPERIMENTAL APPARATUS

Experiments were performed in a recirculation open water channel shown in Fig. 1(a); the flow was circulated by a magnetic drive centrifugal pump (Iwaki, Japan) in a view to avoid structure vibration of the facility. A settling chamber, a honeycomb, 6 screens and a contraction were placed in sequence to ensure flow homogeneity. Dimensions of the test section were 150 mm (width) \times 200 mm (height) \times 1050 mm (length). The free-stream velocity was kept at 0.125 m/s , resulting in a Reynolds number

based on the plate thickness $Re_D=1000$. The free-stream



1. Pump 2. Settling tank 3. Diffuser 4. Settling section 5. Contraction 6. Test section 7. Recycle tank

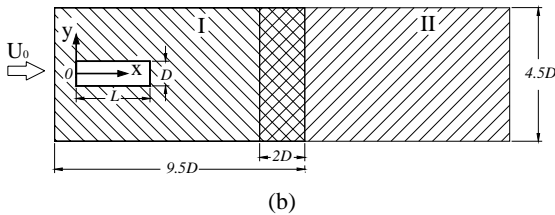


Fig. 1 Schematic of the (a) experimental set-up and (b) measurement regions

turbulence intensity was measured to be less than 2%. The blunt plates with length-to-thickness ratio $L/D = 3, 6, \text{ and } 9$ were placed in the middle depth of the water channel. The selection of the aspect ratios was based on the consideration that each case with different length-to-thickness ratio corresponds to a certain shedding mode (Parker and Welsh, 1983; Nakamura et al, 1991), besides, the first integral L/D of each branch was chosen to avoid two dominant frequencies at the jump.

The velocity field around the plate was measured by using two-dimensional Particle Image Velocimetry (PIV). A CCD camera (IPX 11M, USA) with 4000×2600 pixels was used to acquire images; the image distortion was suppressed by using an 85 mm lens (PC Micro Nikon, Japan). The hollow glass beads ($\rho \approx 1.05 \text{ kg/m}^3$, $d \approx 10 \mu\text{m}$) were used as tracer particles; the flow plane of interest was illuminated by an 1.8W semiconductor laser. The continuous laser was modulated to give 5 ms pulses and synchronized with the CCD camera by using a pulse delay generator. The inherent inter-channel time interval of the generator is the order of pi-second, resulted in a well synchronization of the CCD camera and the laser. The appropriate combination of cylindrical lenses was fitted with the compact laser to produce a 1 mm thick light sheet on the center of the cylinder. As shown in Fig. 1(b), measurements were taken at two adjacent regions ($9.5D \times 4.5D$) for longer plates ($L/D = 6, 9$) by traversing the light sheet and the camera; these two regions were overlapped $2D$ in the streamwise direction for ease of giving a combinative distribution of the time-averaged quantities. One measurement region is enough to cover the region of our interest for short plate ($L/D = 3$). The abscissa corresponds to the streamwise coordinate, x , and the ordinate is the wall normal coordinate, y , both normalized by the plate thickness D . The origin locates at

the center of the front end of the plate. At each measurement region, a total of 500 velocity fields were acquired. The standard cross-correlation algorithm in combination with window offset (Westerweel et al., 1997), sub-pixel recognition by Gaussian fitting (Sugi et al., 2000) and sub-region distortion was used to improve the signal-to-noise ratio. The interrogation window size was 64×64 pixels with a 62.5% overlap. This gave a spatial resolution of 0.47 mm between vectors.

RESULTS AND DISCUSSIONS

To gain a general impression of the flow features, time-averaged streamline patterns are shown in figure 2 with contours of the time-mean streamwise velocity.

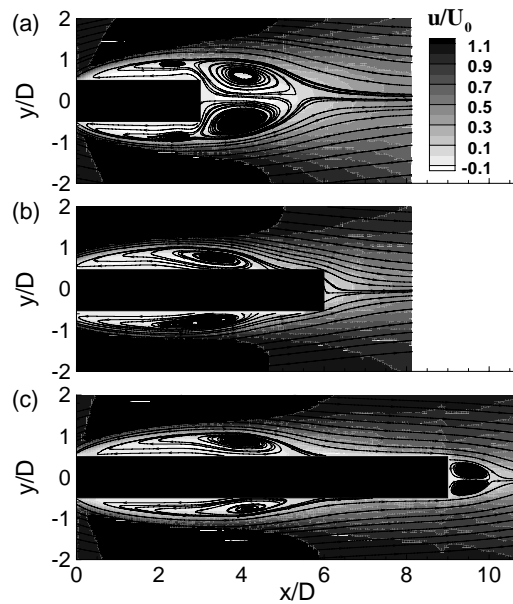


Fig. 2 Time-averaged streamlines and contours of streamwise velocity for $L/D = (a) 3, (b) 6, (c) 9$

Two large recirculation zones are observed in the near wake of the plate for $L/D = 3$ (Fig. 2(a)), the spatial size of the recirculation zone is almost $2D$ in the streamwise direction and $1D$ in the vertical direction. Of particular interest, the recirculation zones are still in conjunction with respective shear layers without detachment. The light contours in the shear layers and wake region indicates that the streamwise velocity is relatively low. The flow patterns for $L/D = 3$ are notably different after an examination of Fig. 2(b) and (c). Two slim time-averaged separation bubbles are found on the opposite sides of the plate for $L/D = 6$ (Fig. 2(b)). The time-averaged reattachment point is nearly $5D$ downstream of the leading edge. Similar distributions are observed in Fig. 2(c), the time-averaged reattachment point is roughly $6D$ downstream of the leading edge. However, two small recirculation zones occur in Fig. 2(c) which is not observed in Fig. 2(b). This is probably due to the redevelopment of the reattached shear layer.

Fluctuation intensities of the streamwise velocity are depicted in Fig. 3; vector plots are also included for ease of explanation. The fluctuation intensity has the highest level

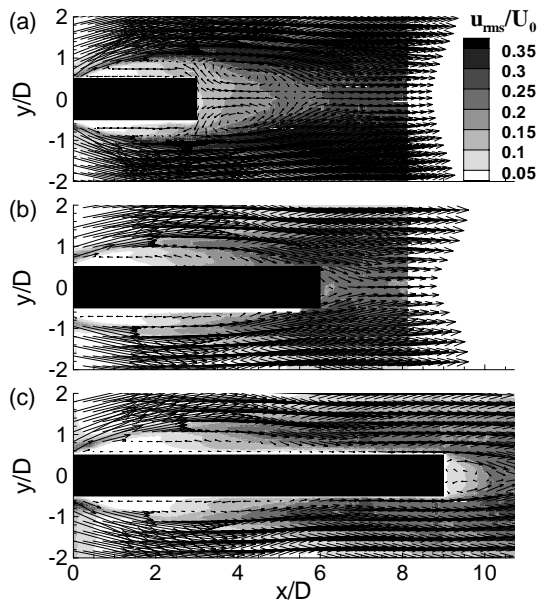


Fig. 3 Vector plot and contours of streamwise velocity fluctuation intensity for $L/D =$ (a)3, (b)6, (c)9

in Fig. 3(a) with a maximum of 35%, indicating the flow in the shear layer is highly unsteady. It is undoubtedly that the shed vortices contribute most to the unsteadiness. Besides, the interaction between the upper and shear layer also make great effect to the unsteady motion. Contours shown in Fig. 3(b) indicate that the flow is less unsteady probably due to the lack of interaction between shear layers. The region of higher level of fluctuation intensity occurs near the trailing edge, where the separated shear layers reattach to the plate's surface. In Fig. 3(c), the region near the reattachment point is also of high level of intensity due to the reattachment and redevelopment of the shear layers.

POD Analysis

To shed more light on the flow structures embedded in the turbulent flow, proper orthogonal decomposition analysis is performed on 500 flow realizations to identify flow structures which contribute to the fluctuating flow energy. The proper orthogonal decomposition (POD) is a technique for extracting a basis for a modal decomposition from an ensemble of signals, and has found enormous applications in many areas under different names such as Karhunen-Loève decomposition, principle components analysis, and empirical eigenfunction decomposition. It was first introduced to the context of turbulence by Lumley (1967) as an analysis technique to identify the coherent structures in turbulent flows, and then the analysis based on POD has been applied to various types of flows (Gordeyev et al., 2000; Rona et al., 2003; Kim et al., 2005; and Gurka et al., 2006). The proper orthogonal decomposition extracts the most energetic eigenmodes by retaining only a small number of modes that capture most of the fluctuation energy. The PIV technique allows acquisition of sequential velocity data at a large number of spatial points simultaneously, and so it provides an attractive basis for POD (Kim et al., 2005).

The general goal of POD is to find the optimal representation of the field realizations. The problem results in solving a two-point correlation matrix. In order to reduce the computational effort involved in solving the eigenvalue problem, the snapshot method was introduced by Sirovich (1987). For simplicity, please refer to Sirovich (1987) and Kim et al. (2005) for detailed mathematical reduction of POD.

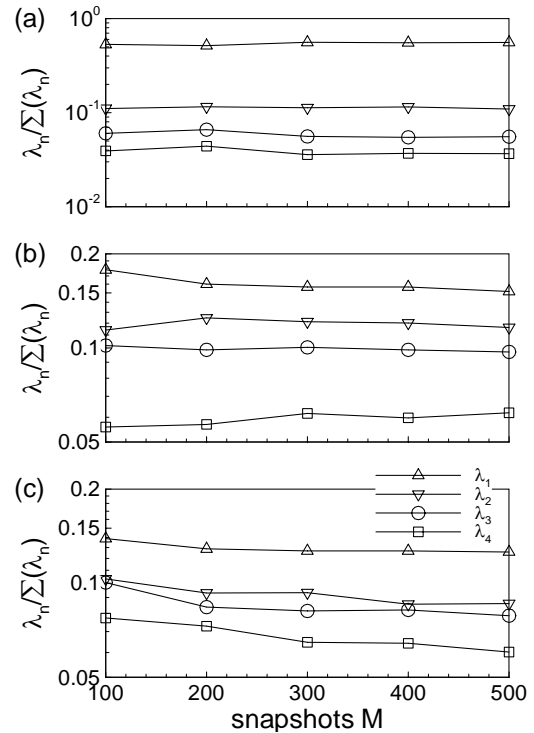


Fig. 4 Test of independence on snapshot number for $L/D =$ (a)3, (b)6, (c)9

The sensitivity of the POD analysis results in relation to the ensemble size M has been tested for each case by using data subsets of different size (Oudheusden et al., 2005). The results (Fig. 4) reveal that the magnitude of the largest eigenvalues does not change significantly for M larger than 200, indicating that the present ensemble size is sufficiently large for providing statistically converged results.

Fig. 5 displays the relative contributions of the single POD modes. It can be observed that the contributions of the lower order eigenmodes are relatively higher than that of the following. Besides, the contributions of the low-order modes in case $L/D = 3$ are greater than that of $L/D = 6$, and 9. As shown in Fig. 5, the relative energy for the first two modes is nearly 20% and 15% respectively for $L/D = 3$, while it is below 10% for $L/D = 6$, and 9, indicating that the large scale structures are more dominant in case $L/D = 3$. The interaction of the shear layers in the wake disappeared for $L/D = 6$, and 9, thus no dominant vortical structures were shed. The contributions of the single modes decrease very rapidly for the first several eigenmodes, and then keep at very small values thereafter. Thus the convergence of the cumulative flow energy towards 100% is relatively slow.

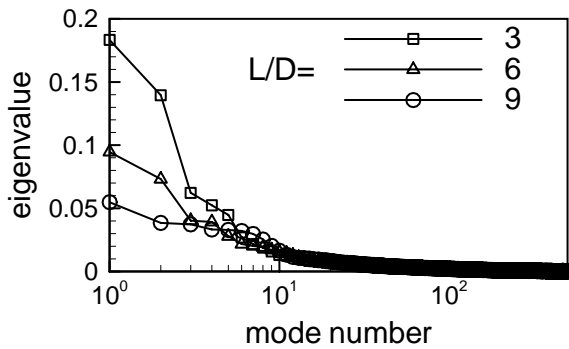


Fig. 5 Distribution of eigenvalues

Fig. 6-8 shows the vector plots of the selected eigenmodes. In Fig. 6, the first eigenmode is the most dominant structure, and has the largest spatial size. With the increase of the mode order, the relative energy is reduced, and also the spatial size of the modes decreases. Interestingly, one vortex was observed in the 1st mode and two vortices in the 2nd mode. The 3rd and 4th eigenmode seems to occur in pairs with symmetrical configuration along the central line of the plate. As pointed out by Sirovich (1987), these coherent structures are not necessarily the coherent structures found in experiments, the physical meaning of these modes remain to be standstood.

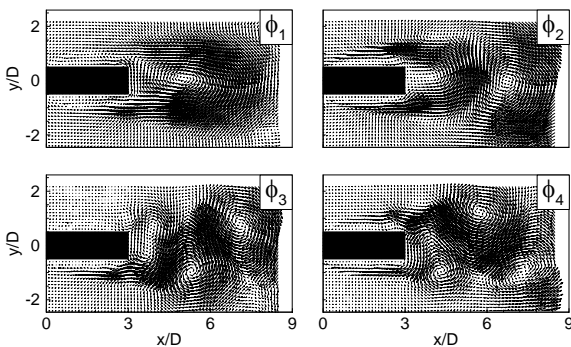


Fig. 6 Selected eigenmodes for L/D=3

Fig. 7 reveals that the most energetic modes in the flow are the large scale structures in the wake as shown in Fig. 7(a) and (b). The vortical structures in the shear layers are less energetic with smaller spatial size.

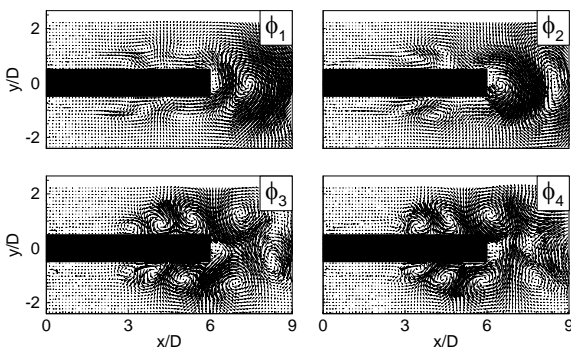


Fig. 7 Selected eigenmodes for L/D=6

The 1st mode shown in Fig. 8(a) for L/D = 9 indicates that the most energetic structure is the reverse flow in the separation bubble. However, this flow structure is not much dominant with only 5% of the fluctuating flow energy. The 2nd, 3rd and 4th eigenmode indicates certain type of vortical structures.

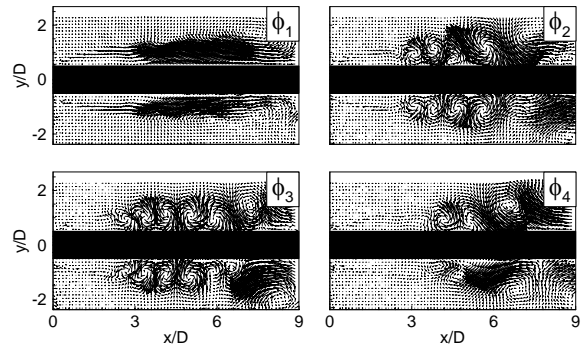


Fig. 8 Selected eigenmodes for L/D=9

CONCLUSIONS

PIV measurements were performed on finite blunt plates at Reynolds number $Re_D=1000$. The length-to-thickness ratios of the plates tested were 3, 6, and 9, respectively. It was found that the separated shear layers interact in the wake without reattachment onto the plate's surface, forming two large recirculation zones. The time-averaged reattachment point was found near the trailing edge of plate for L/D = 6, while it was far upstream for L/D = 9. The flow is highly unsteady for L/D = 3 due to the strong interaction of the shear layers in the wake which lead to large scale vortex shedding. The interaction was eliminated for longer plates as L/D = 6, and 9. The distribution of eigenvalues demonstrated the overwhelming dominance of the large scale structures for L/D = 3. Selected eigenmodes showed that these three cases were featured by different flow structures.

REFERENCES

Gordeyev, S.V., and Thomas, F.O., 2000, "Coherent structures in the turbulent planar jet. Part 1, Extraction of proper orthogonal decomposition eigenmodes and their self-similarity", *Journal of Fluid Mechanics*, Vol. 414, pp. 145-194.

Gurka, R., Liberzon, A., and Hetsroni, G., 2006, "POD of vorticity field: A method for spatial characterization of coherent structures", *International Journal of Heat and Fluid Flow*, Vol. 27, pp. 416-423.

Hourigan, T., Thompson, M.C., and Tan, B.T., 2001, "Self-sustained Oscillations in Flows around Long Blunt Plates", *Journal of Fluids and Structures*, Vol. 15, pp. 387-398.

Kim, Y., Rockwell, D., and Liakopoulos, A., 2005, "Vortex buffeting of aircraft tail: interpretation via proper orthogonal decomposition", *AIAA Journal*, Vol. 43, pp. 550-559.

Lumley, J.L., 1967, "The structure of inhomogeneous turbulence", In *atmospheric turbulence and wave*

propagation. ed Yaglom AM, Tatarski VI, 166-178.

Mills, R., Sheridan, J., and Hourigan, K., 2003, "Particle Image Velocimetry and Visualization of Natural and Forced Flow around Rectangular Cylinder", *Journal of Fluid Mechanics*, Vol. 478, pp. 299-323.

Nakamura, Y., Ohya, Y., and Tsuruta, H., 1991, "Experiments on Vortex Shedding from Flat Plates with Square Leading and Trailing Edges", *Journal of Fluid Mechanics*, Vol. 222, pp. 437-447.

Ohya, Y., Nakamura, Y., Ozono, S., Tsuruta, H., and Nakayama, R., 1992, "A Numerical Study of Vortex Shedding from Flat Plates with Square Leading Trailing edges", *Journal of Fluid Mechanics*, Vol. 236, pp. 445-460.

Parker, R., and Welsh, M.C., 1983, "Effects of Sound on Flows Separation from Blunt Flat Plates", *International Journal of Heat and Fluid Flow*, Vol. 4, pp. 113-127.

Rona, A., and Brooksbank, E.J., 2003, "POD analysis of cavity flow instability", AIAA paper 2003-0178.

Sirovich, L., 1987, "Turbulence and the dynamics of coherent structures", *Quarterly of Applied Mechanics*, Vol. 45, pp. 561-571.

Sugii, Y., Nishio, S., Okuno, T., and Okamoto, K., 2000, "A Highly Accurate Iterative PIV Technique Using A Gradient Method", *Measurement Science and Technology*, Vol. 11, pp. 1666-1673.

Van Oudheusden, B.W., Scarano, F., Hinsberg, N.P.V., and Watt, D.W., 2005, "Phase-resolved characterization of vortex shedding in the near wake of a square-section cylinder at incidence", *Experiments in Fluids*, Vol. 39, pp. 86-98.

Westerweel, J., Dabiri, D., and Ghacylinder, M., 1997, "The Effect of A Discrete Window Offset on The Accuracy of Cross-correlation Analysis of Digital PIV Recordings", *Experiments in Fluids*, Vol. 23, pp. 20-28.